Biosonar Responsivity Sets the Stage for the Terminal Buzz

Ravi Umadi[1] Uwe Firzlaff[1]

[1] Lehrstuhl für Zoologie, TUM School of Life Sciences, Technische Universität München, Liesel-Beckmann-Str. 4, 85354, Freising-Weihenstephan, Germany

Abstract. Echolocating bats must continuously adapt their sonar output to meet the increasing demands of prey pursuit. While call rate and duration modulations have been extensively described, the underlying control thresholds governing these transitions remain poorly understood. Here, we present a predictive framework based on a novel metric *responsivity*, defined as the inverse change in interpulse interval (IPI), to quantify moment-to-moment temporal precision in sonar control. This metric reveals a critical transition point—*buzz readiness*—where fine-scale IPI adjustments peak prior to the onset of the terminal buzz. By integrating biologically plausible reaction time constraints with echo-acoustic feedback loops, our model predicts how increasing relative velocity compresses the time available for sonar adaptation. Simulations incorporating prey motion and bat flight kinematics reproduce a consistent sub-linear tradeoff between call rate and relative velocity. High-resolution field recordings from a portable, custom-built microphone array validate the model predictions, demonstrating that buzz readiness thresholds reliably align with behavioural transitions in natural prey interception. The framework further explains why shortened or absent buzzes occur at high velocities, when reaction constraints prevent full transition into the buzz phase. This work introduces a generalised, predictive model linking sensory-motor control, kinematics, and temporal adaptation in bat biosonar. The responsivity approach offers new tools to quantify control dynamics in natural behaviour and provides a foundation for biologically inspired sensing systems operating under real-time constraints.

Keywords: Echolocation dynamics, Prey interception, Relative velocity, Sonar, Responsivity, Terminal buzz, Predator-prey interactions

1 INTRODUCTION

Echolocating bats exemplify the sophistication of active sensory systems, where the dynamic and rapid behavioural adaptations have long been recognised as central to navigating the environment and intercepting prey [1–4]. An echolocating bat emits short, high-frequency calls, listens to the echoes to obtain information about its surroundings and to orient and adjusts the call and behavioural parameters as necessary. When a target is detected, the bat approaches it and transitions into shorter and more frequent calls. A successful interception is assumed to be characterised by a rapid succession of calls at up to 200 calls per second at the end—a phenomenon known as *terminal buzz*. Field and laboratory studies have established that the echolocating bat modulates every parameter of the acoustic response as the context demands [5–9]. A key insight from studies of other predator–prey systems is the importance of speed and reaction time in successful hunting. This has been well characterised in cursorial predators like cheetahs chasing antelopes [10]. However, it remains underexplored in volant predators such as bats. Other than the crucial calling frequency adaptations in response to the Doppler effect in constant frequency call emitters [11–15], this fundamental physical parameter has received comparatively little attention.

Corresponding author: Ravi Umadi– Email: ravi.umadi@tum.de

SUMMARY. In this study, we introduce a new way to understand how bats control their echolocation behaviour as they pursue prey. Bats emit sonar calls and listen to returning echoes to track their environment, but how they adapt their call patterns in real-time as they approach targets has remained poorly understood. Rather than focusing only on how fast bats call, we developed a novel metric called *responsivity*, which captures how precisely bats adjust their call timing from one pulse to the next. This measure helps identify the moment when bats prepare to enter their final rapid call phase — known as the terminal buzz — which marks the last stage of prey capture.

We developed a first-principles mathematical framework and built a computational simulation to understand the echolocation behaviour of actively foraging bats. Our model predicts how bats adapt their call rate based on their relative speed to prey, showing that faster approaches compress the time available for sensory updates, sometimes leading to shorter or missing buzz sequences. To validate the model, we analysed both synthetic simulations and high-resolution field recordings from free-flying bats, using custom-built microphone arrays to capture full call sequences and flight trajectories.

The results showed that the predicted responsivity peaks and reaction time limits closely match the field data, and that the transition to the buzz phase can be reliably detected from call timing alone. Furthermore, we found that both simulated and real-world data follow a consistent power-law relationship between call rate and approach velocity, reflecting a trade-off between sensory update rate and kinematic demands. This predictive framework provides a new understanding of how bats regulate sonar behaviour under time pressure and offers tools for studying dynamic sensory systems more generally.

Recent work by Jakobsen et al. (2025) [16] demonstrated that echolocation behaviour in aerial-hawking bats is more closely regulated by flight velocity than by absolute prey distance. Their findings underscore the role of temporal parameters in shaping kinematic decision-making, suggesting that precise call timing is central to sensory-motor coordination. However, while the study elevates the importance of velocity in echolocation control, it stops short of providing a mechanistic or predictive framework for how velocity drives adaptations in sonar behaviour during interception tasks.

As extensively as echolocation research has been over the decades, a generalised mathematical model and predictive framework have remained elusive.

The pace at which predator-prey interactions play out further compels understanding of the time sequence of actions and events in a racing system of rapid sensory-motor calibrations with evolving strategies. The time beacons of the echolocation calls make the system particularly amenable to temporal delineation, with which the limits of the system parameters may be revealed.

One such characterisation is the rate at which the changing parameters adapt to demanding contexts, a function we introduce as *responsivity*, which we incorporate in a mathematical framework that formalises the relationship between call rate, echo delay, relative velocity, and use it to deduce the limit of the biological reaction time of the echolocating animals. By treating sonar responsivity as a measurable function of the temporal dynamics between call emission and echo arrival, we derive a novel limit - termed *buzz readiness* - beyond which further increases to call rate adaptations offer no additional sensory-motor advantage.

The central hypothesis of this work is that the relative velocity between the bat and its target governs the emergence of interception strategies via a tradeoff between speed and sonar update rate. At higher relative velocities, the system reaches its reaction threshold closer to the target, often constraining or eliminating the production of a long terminal buzz. At lower velocities, the responsivity peak is reached earlier, permitting extended call rate acceleration and facilitating a full buzz. This tradeoff predicts behavioural outcomes, such as capture success or abandonment, and reveals how echolocation call dynamics are tuned to optimise sensory acquisition within a velocity-bounded temporal envelope.

To validate the insights provided by this framework, we developed a simulated echolocation system that mimics the real-world phenomenon and offers the advantage of tuning behavioural parameters to study the outcomes. Further, we recorded foraging wild bats with a microphone array and calculated acoustic, kinetic and behavioural parameters to verify the hypotheses. Our results proved the theoretical framework and show that the interception strategies evolve due to the velocity-call rate tradeoff, where the innate biological limits play a central role. The results of the experiments by Geberl et. al. (2015) [6], where they systematically measured the sensory reaction timings by removing the prey at different times-before-contact to establish the point where bat would not be able to react to the removal of the prey— by not being able to abandon capture attempts and the terminal buzz— further give credence to our framework.

By formalising the constraints of sonar responsivity and introducing the concept of buzz readiness, this work establishes a predictive framework for understanding how interception strategies emerge from movement-perception tradeoffs. The combination of generative simulation and high-resolution field recordings enables a mechanistic understanding of biosonar dynamics under naturalistic constraints. In doing so, this study not only refines our interpretation of buzz behaviour but also lays the groundwork for generalising these principles across sensory systems where biological latency and physical relative motion co-shape perception and action.

2 METHODS

2.1 Sonar Temporal Responsivity and Reaction Times

The responsivity metric $\mathcal{R}$, defined as the inverse of the change in interpulse interval (IPI), captures more than just the magnitude of temporal adaptation; it quantifies the echolocation system's capacity for fine motor control under increasing sensory demands. As the bat approaches a target, its IPIs shrink progressively, reflecting a rising need to update sonar information more frequently. However, $\mathcal{R}$ does not peak when the call rate is highest; rather, it peaks when the bat begins to make the *smallest possible adjustments* in IPI to continue adapting its call rate. In this regime, even minute changes in IPI reflect substantial control effort–the finer control and coordination efforts being more demanding than coarser control efforts [17]. Thus, $\mathcal{R}$ is not a measure of speed, but of sensitivity – how delicately the bat can tune its sonar output in response to a rapidly evolving scene.

This behaviour is analogous to fine motor control in other biological systems: when the system begins operating near its physiological limits, it must exert greater control to maintain stability and precision. A high value of $\mathcal{R}$ implies that the bat is entering a state where temporal motor control is maximally engaged - where the *ability* to make small changes in timing becomes crucial to avoiding echo-call overlap, maintaining sensory coherence, and preparing for the imminent

need to emit pulses at the maximum call rate. Therefore, we interpret the peak in $\mathcal{R}$ as the onset of *buzz readiness*: the point at which the bat's sonar system is fully mobilised to deliver its fastest, most focused interrogation of the environment. It is not the maximum call rate itself that defines this threshold, but the ability to make the smallest changes required to achieve that rate – an anticipatory signal that the terminal buzz is near (See the mathematical definition in Section 2.1.3.).

2.1.1 Call Events and Reaction Constant k_r

To estimate the theoretical lower bounds of biological reaction time in echolocating bats, we modelled the timing dynamics between emitted calls and their returning echoes as a function of target distance and sound propagation (see figure 1a). The acoustic travel time, denoted as T_a, was defined as the two-way delay between a call emission and its echo return, accounting for the bat's own displacement during this interval:

$$T_a = \frac{2d(t) - \Delta s}{c} \tag{1}$$

Where $d(t)$ is the instantaneous distance to the target, Δs is the displacement of the bat during sound travel, and c is the speed of sound in air. The total interval between two call emissions Δt (IPI) is composed of T_a and the bat's biological reaction time window T_b, modeled as a proportional function of T_a:

$$T_b = k_r \cdot T_a \tag{2}$$

Here, k_r is a dimensionless biological reaction constant that scales the available reaction time window with respect to echo delay. It corresponds to the entire sensory-motor processing time, from echo reception to subsequent call emission. The call rate C_r is then calculated as the inverse of the total interval:

$$C_r = \frac{1}{T_a + T_b} = \frac{1}{T_a(1 + k_r)} \tag{3}$$

2.1.2 Call Duration Contraction Threshold

As the bat approaches its target, the acoustic travel time (echo delay) between call emission and echo reception decreases. To avoid overlap between outgoing calls and returning echoes, the bat must reduce the duration of its calls in accordance with the shrinking echo delay. This necessity defines a threshold for call duration contraction, governed by the inequality:

$$t_{\text{call}} < T_a + T_{b^*} \tag{4}$$

where t_{call} is the emitted call duration, and T_{b^*} is the fastest biological reaction time (See Equation 9). The distance at which this inequality becomes critical can be used to estimate the spatial onset of call duration decrement.

To determine this distance threshold, the inequality can be rearranged as:

$$d_c = \frac{t_{\text{call}} \cdot c}{2} + T_{b^*} \cdot v \tag{5}$$

where d_c is the critical distance at which call duration contraction must begin, and v is the bat's relative velocity. Figure 1d illustrates how this threshold varies for different values of the

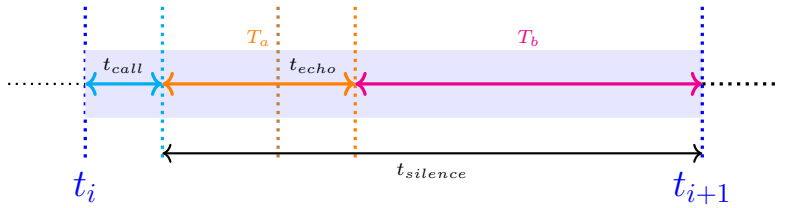

(a) Call Event Model

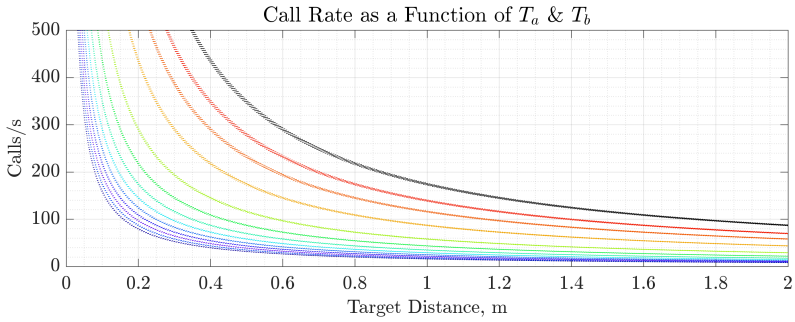

(b) Call Rate Limit At Decreasing Target Distances

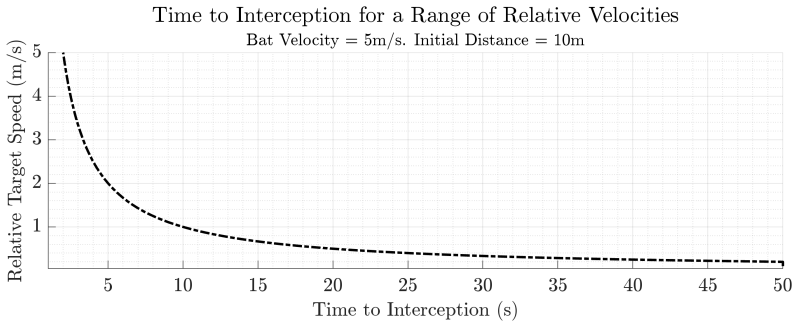

(c) Time to Interception

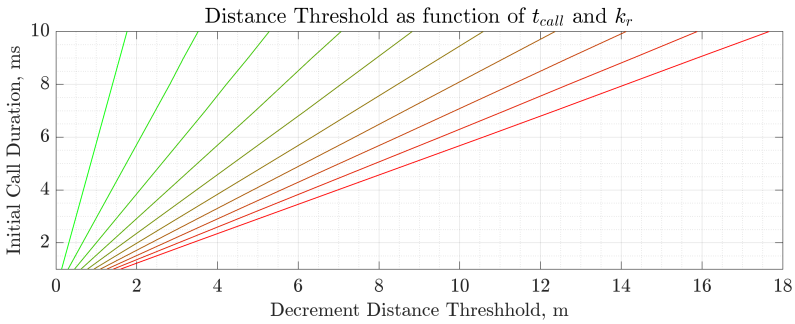

(d) Call Duration Decrement Model

Figure 1: Temporal Parameters and Limits (**1a**) The time window for call duration decreases as the acoustic travel time decreases with the progressing approach, reaching the limit of T_b. The call sequences continue as may be expressed by $[t_i, t_{i+1} ... t_N] = \bigcup_{n=1}^{N} [T_a, T_p, T_r, T_l]^n$, where the processing ($T_p$), response ($T_r$) times sum up to T_b, and lag (T_l) is considered zero. (**1b**) The call rate of an actively foraging bat pursuing a target. In this model, we calculate the call rate as a function of ratios of T_a and T_b as call rate, $r_c = 1/(T_a + T_b)$, where, $T_b = (k_r \cdot T_a) \rightarrow k_r$: 0, 0.25, 0.5, 1, 2, ...10, colour-coded from black to dark blue. Each ratio is calculated for subject velocity v, ranging from 1 to 10m/s. The lower limit of T_b, the shortest lag with the fastest processing time, can be interpreted based on empirical maximum call rates and k_r. (**1c**) Modelling interception time as a function of relative velocity. (**1d**) For a given initial call duration, the distance at which $t_{call} \approx T_a + T_{b*}$ is colour-coded for k_r=1:10 (green to red) at 5 m/s.

reaction constant k_r, which modulates T_b as a multiple of T_a.

In the simulation, the bat reduces its call duration when the current target distance $d(t)$ falls below the calculated contraction threshold. This dynamic ensures that emitted calls do not interfere with echo processing, especially during the final phases of the approach. The onset of call duration contraction, when mapped alongside the moment of target detection and the point of maximum responsivity, provides insight into how bats temporally coordinate their vocal and perceptual systems for successful interception (See Figure 6).

2.1.3 Responsivity and Reaction Time Thresholds

To quantify the temporal sharpness of adaptation during echolocation, we define a metric called *responsivity*, which reflects the bat's capacity to make precise, moment-to-moment changes in its interpulse interval (IPI) as target distance decreases. This measure captures not only how rapidly the bat is increasing its call rate, but more importantly, how *finely* it can adjust sonar timing in anticipation of the terminal buzz.

We define the IPI at call index n as:

$$\Delta t_n = t_{n+1} - t_n, \tag{6}$$

where t_n is the timestamp of the n-th call.

Responsivity at index n is defined as the inverse of the change in IPI magnitude between successive calls:

$$\mathcal{R}_n = \left| \frac{1}{\Delta t_{n+1} - \Delta t_n} \right|. \tag{7}$$

This formulation gives high responsivity values when the system begins making very small changes in IPI - indicative of the bat engaging maximal temporal precision. As such, $\mathcal{R}_n$ acts as a proxy for the system's dynamic readiness: the smaller the IPI change, the more sensitive and responsive the sonar output becomes. The metric captures a control regime where the bat avoids both sensory interference (echo-call overlap) and premature saturation of its maximum call rate.

To identify the onset of this transition, we compute $\mathcal{R}_n$ across the sequence and determine the index at which it is maximal:

$$n^* = \arg\min_n |\mathcal{R} - C_{r_{\max}}| \tag{8}$$

This index n^* marks the moment of peak sonar responsivity, which we define as the *buzz readiness point*—the call at which the bat's sonar system is fully engaged to enter the terminal buzz.

To quantify the sharpness of adaptation at this transition, we define the *fastest reaction time* T_{b^*} as the absolute difference in IPI across the buzz readiness index:

$$T_{b^*} = |(\Delta t_{n^*+1} - \Delta t_{n^*})| \tag{9}$$

This value captures how quickly the bat is compressing its sonar output at the inflexion of control. A small T_{b^*} reflects a rapid acceleration into the buzz phase, whereas a larger T_{b^*} suggests a more gradual transition.

We interpret the pair $(\mathcal{R}_{n^*}, T_{b^*})$ as defining the bat's sensorimotor posture at the moment

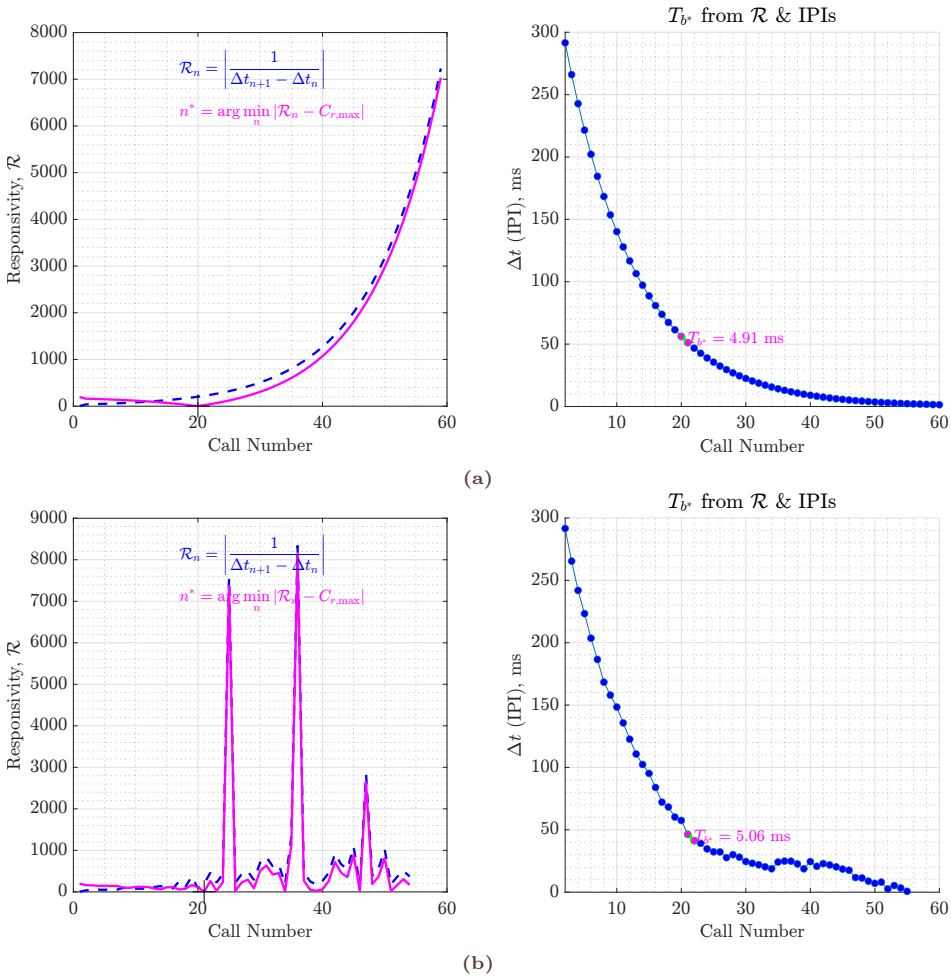

Figure 2: Absolute deviation of responsivity $\mathcal{R}_n$ from the physiological call rate limit ($C_{r,max} = 200$ Hz) and T_{b^*} The two simulated scenarios - stationary (**Top**) and motile prey (**Bottom**). The inflexion point corresponds to the minimum of this curve (magenta line), where the system reaches maximal temporal sensitivity, marking the buzz readiness threshold. This minimum reflects the moment at which the bat must begin to exert its finest control to continue adapting sonar output without exceeding physiological constraints. In real-world conditions, the bat may approach this inflexion point and reset, depending on the target.

of commitment to buzz initiation. This allows for a computationally efficient and biologically grounded method to infer buzz readiness from call timing alone—whether in simulated or field-recorded data.

Finally, we note that this method is robust to the absolute values of IPIs or call rate, focusing instead on the pattern of change and the sensitivity of adaptation. As such, it can be generalised across individuals and species with differing physiological limits, provided a reasonable upper bound on call rate is known.

2.2 Responsivity as Predictive Control Threshold

During an approach, the call rate increases gradually at first, followed by an exponential rise as the bat approaches its maximum emission rate. However, the point of maximum responsivity is not the peak call rate. Instead, it occurs earlier, at a point where the system begins making the smallest possible adjustments in IPI. This point marks the inflexion in the control curve: before this, the sonar system is adjusting at relatively coarse scales; after this, it enters a regime of

fine-grained motor timing (Figure 2).

The responsivity curve $\mathcal{R}_n$ rises sharply at the transition into this regime, capturing the onset of the most constrained, reactive control behaviour. Importantly, this transition occurs well before the call rate saturates, indicating that the sonar system begins preparing for maximum output in advance of reaching its physiological limit. In other words, the system does not react to hitting the maximum call rate – it anticipates its approach by increasing its temporal precision.

This anticipatory mechanism suggests that the responsivity peak represents a biologically meaningful control threshold. The bat transitions into the buzz not when it is forced to emit pulses rapidly, but when it detects that doing so will soon become necessary. This proactive control posture aligns with principles observed in other motor systems, where fine adjustments are recruited under heightened task demands [18].

2.3 Simulated Foraging Call Sequence

The simulation implements a dynamic model of an echolocating bat pursuing a target while adapting its call rate and duration based on proximity and echo feedback. The simulation iteratively updates sonar parameters based on the bat's forward velocity and estimated echo delay. We implemented simulations for a typical FM bat and a CF bat.

Parameter Initialization

The simulation was initialised with a set of physical and signal-specific parameters chosen to reflect biologically plausible conditions for an actively foraging bat. The speed of sound in the air was set to $c = 343\,\mathrm{m/s}$ (to avereage summer temperatures 20°C at 520 m asl. at the field study location), and the initial distance between the bat and the target was defined as $d_0 = 20\,\mathrm{m}$. The bat's forward velocity was initialised to a desired value for the run, with each echolocation call having an initial duration of $t_{\mathrm{call}} = 5\,\mathrm{ms}$. The maximum allowable call rate in the simulation was set to $R_{c_{max}} = 200\,\mathrm{calls/s}$, constrained by the known physiological capabilities of vespertilionid bats [19]. A biological reaction constant of $k_r = 5$ was chosen by referring to the call-rate to k_r correspondence (Figure 1a) to scale the interpulse interval relative to the echo delay. Atmospheric attenuation was modelled as a frequency-dependent function $\alpha(f, T, H)$, which accounts for the influence of ambient temperature and humidity. Finally, the initial source level of the emitted calls was set to a standard reference value of 94 dB SPL.

The constant frequency bat echolocation simulation was run with the same conditions, including k_r for comparibility, except for the initial call duration (50ms), maximum call rate (100Hz) and the target distance of 60m - where the higher distance value was necessary to extract the full event parameters of the model; otherwise, the point of target detection would have been omitted.

In the runs to simulate a motile prey, we introduced a random shift in relative target position with ±10 cm with each call, thus introducing corresponding adaptation to downstream parameters.

Echo and Interpulse Timing

The interpulse interval (IPI) is modelled using the reaction time constant:

$$\Delta t(n+1) = k_r \cdot T_a(n+1) \tag{10}$$

The echo reception time is:

$$T_{\mathrm{e}}(n+1) = \sum_{i=1}^{n+1} \Delta t(i) + T_a(n+1) \tag{11}$$

Target Update Based on Forward Displacement

Assuming constant bat velocity, the forward displacement per call is computed as:

$$\Delta s(n) = v_{\mathrm{bat}} \cdot \Delta t(n+1) \tag{12}$$

This distance is subtracted from the previous target range:

$$d(n+1) = d(n) - \Delta s(n) \tag{13}$$

This sequence continues until the target distance becomes zero or negative, indicating interception. In the runs simulating a motile prey, a random value between -0.1 and 0.1 was added to Δs, which simulated a variable relative velocity (See Figure 10).

Echo Level and Detectability

For each echolocation event, the simulation models the received level of the echo signal based on the bat's distance to the target and the acoustic environment. The target strength $TS(n)$ is computed as a function of the call frequency, the target's effective diameter, and the distance at the $(n+1)$-th call, incorporating frequency-dependent atmospheric attenuation $\alpha(f, T, RH, P)$:

$$TS(n) = f_{\mathrm{TS}}\left(f_{\mathrm{min}}, D_{\mathrm{target}}, d(n+1), \alpha\right) \tag{14}$$

To account for signal loss during propagation, the model includes geometric spreading attenuation $TL(n)$, calculated as a round-trip loss:

$$TL(n) = 2 \cdot f_{\mathrm{geom_atten}}(d(n+1)) \tag{15}$$

The received level $RL(n)$ at the bat's ears is then given by:

$$RL(n) = SL - |TL(n)| + TS(n) \tag{16}$$

where SL is the emitted source level. If the received level falls below a defined detection threshold, the echo is considered undetectable. This threshold condition enables the simulation to determine the point of target detectability during the approach. These calculations allow the system to dynamically assess whether each returning echo is strong enough to inform further motor actions or call adjustments.

Simulation Output

The simulation output is a time-resolved sequence of acoustic and spatial parameters characterising the approach of a bat toward a target under biologically plausible conditions. The primary output includes a vector of echo delays, interpulse intervals, and updated target distances at

each echolocation event. As the bat moves forward, the simulation dynamically updates the time of flight for each echo, the time until the next call, and the new distance to the target based on the bat's velocity and processing delay. This time-series data simulates how the echolocation behaviour unfolds during a prey pursuit, with decreasing distances, shortening delays, and increasing call rate as the bat nears its target. Additionally, the received signal level (RL) at each step is computed by accounting for both geometric spreading and atmospheric attenuation, along with the target's echo strength. If the received level drops below the detection threshold, the call is considered undetectable, allowing the simulation to also evaluate conditions under which the bat may lose acoustic contact with the target. Together, these outputs form a full temporal profile of the sonar feedback loop, enabling downstream analysis of responsivity, buzz onset, and interception strategy as functions of relative velocity and detection reliability.

A custom MATLAB function was implemented to generate biologically realistic echolocation calls. This function synthesises individual bat calls using a linear frequency-modulated (FM) down-sweep, which is characteristic of vespertilionid bat echolocation (Figure 4b). Each call starts at a higher frequency f_1 and sweeps down to a lower frequency f_0 over a duration d, sampled at rate fs. The function applies a Hanning window to taper the signal smoothly at both ends, minimising spectral artefacts. The synthesised waveform represents a single echolocation event and is appended to a temporal sequence following the obtained interpulse intervals. For each simulated call in the foraging sequence, a corresponding echo waveform is generated and temporally aligned. This results in a complete audio stream of alternating call and echo segments.

This framework provides a simplified yet quantitatively rich model for simulating call sequences under realistic foraging conditions and evaluating the effects of forward motion on sonar dynamics.

2.4 Interception Strategy Based on Relative Velocity

A key component of the theoretical model developed in this study is the hypothesis that prey interception behaviour in echolocating bats is governed by the relative velocity between the bat and its target. This relative velocity, defined as $v_r = v_{\text{bat}} - v_{\text{target}}$, determines the time window available to complete the sensory-motor loop necessary for successful capture. Assuming the bat emits a call at an initial distance d_0 from the target, the time to interception is given by:

$$t = \frac{d_0}{v_r} \tag{17}$$

This inverse relationship forms a rectangular hyperbola (Figure 1c & 6), such that small relative velocities lead to extended interception durations, while higher relative velocities shorten the time available for sonar updates, leading to distinct behavioural outcomes:

$$\begin{cases} v_r = 0 & \Rightarrow \text{chase time } \to \infty \\ v_r \ll v_{\text{bat}} & \Rightarrow \text{long, prominent buzz} \\ v_r \approx v_{\text{bat}} & \Rightarrow \text{short buzz} \\ v_r \gg v_{\text{bat}} & \Rightarrow \text{no buzz} \end{cases} \tag{18}$$

In this context, the buzz, defined as a rapid sequence of short, high-rate calls preceding capture, acts as a behavioural manifestation of the highest sonar responsivity. When v_r is small, the bat has ample time to accelerate its call rate and achieve maximum responsivity well

before reaching the target, producing a long buzz. As v_r increases, the bat must reach peak responsivity closer to the target, reducing the length or likelihood of a buzz. In extreme cases where the relative velocity is very high, the adaptation time required to reach the responsivity ceiling may exceed the time to contact, resulting in a complete omission of the buzz. This hypothesis reframes buzz behaviour as an emergent outcome of the dynamic interplay between motion, sensory processing constraints, and environmental predictability. It implies that buzz duration and its occurrence are context-dependent, adapting to the bat's ability to update its spatial model of the target within the confines of echo delay and processing time. This hypothesis is examined through both simulations and field data in subsequent sections.

2.5 Field Data Collection and Analysis

We collected acoustic data to validate the simulation predictions using a four-channel microphone array in a natural foraging environment (Weihenstephan, Freising, Germany, August - September 2021).

The schematic diagram of the setup is shown in Figure 3. An assembled array of four microphones was installed in the indicated position, marked in numbers. The three arms of the array were made of straight wooden strips with a 2 cm square profile. A triangular junction crafted out of wood held the arms in position. The arms could be slipped out by loosening the junction fastener, thus making the setup portable. The junction was mounted on a ball joint as a provision for angular positioning of the array, if necessary. All the surfaces on the array were covered in absorptive foam.

The array was mounted on a studio lighting tripod, extendable up to 3 m, providing enough ground clearance and reaching high enough to face the foraging bats.

The microphones (custom-designed with Knowles SPU0410LR5H-QB) were calibrated against a $\frac{1}{4}''$ B&K reference, and the recording program included a frequency domain signal calibration filter to convolve the incoming signal before writing to uncompressed `.wav` files. The system was powered by 12 v car batteries with a DC-AC inverter supplying the computer and the audio interface. Our recording program included a method to trigger the recording based on signal monitoring, and a recording extension was incorporated to extend the recording if there was call activity in the final seconds of the initially set ceiling of 10 s.

High-quality bat activity sequences were selected based on a signal-to-noise ratio (SNR) threshold of 30 dB. Of over 380 sequences, 35% contained at least one buzz. Extracted calls were manually verified and processed to exclude extracted ground reflections and low SNR calls.

Localisation and flight trajectory reconstruction were performed using a custom MATLAB class, and call parameters (e.g., rate, duration, amplitude), 3D positions and bat velocity profiles were computed. We used the Time Of Arrival Delay (TOAD) method to localise the sound source in 3D. Further quality control was implemented to exclude localisation data points exceeding 8m in any direction, as localisation confidence reduces at increasing distances.

Statistical Analysis and Model Comparison

Power-law regression was applied to simulation and field data to assess the velocity and call rate relationship. A clustering algorithm (DBSCAN) [20] was used to examine the density and distribution of data points in the velocity-call rate domain–implemented using `dbscan` function

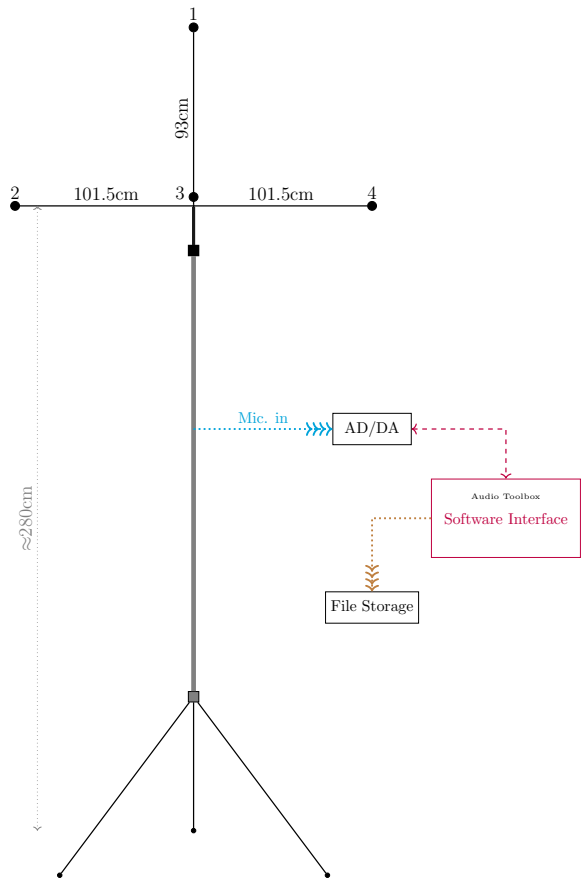

Figure 3: Experimental Setup. We custom-built a microphone array for easy deployment and high-quality recordings. Four custom-designed Knowles MEMS microphones were calibrated against B&K reference microphones, and the incoming signal was convolved with a calibration filter before writing to the disk.

in Matlab. Sparse regions in the upper diagonal domain were flagged as areas where high velocity and high call rates rarely co-occurred.

The model's prediction of buzz readiness timing and its dependence on relative velocity were compared against the field-recorded data to validate the alignment between theory and observation.

All data analysis and visualisation were performed using MATLAB R2023b.

3 RESULTS

We present the results of the simulated echolocation runs in combination with the results of the field data analyses. The combined approach allowed us to test the hypotheses resulting from the first-principle deduction of echolocation behaviour (Figure 1, 2) in tandem with the field data and fit the prediction of the mathematical framework to the field recorded echolocation behaviour of the bats.

Figure 4a presents two example call sequence recordings from the field experiments, from two different species commonly found in the region. The precise species identification was not relevant to the analysis; therefore, it was not attempted. The call sequences end in a terminal

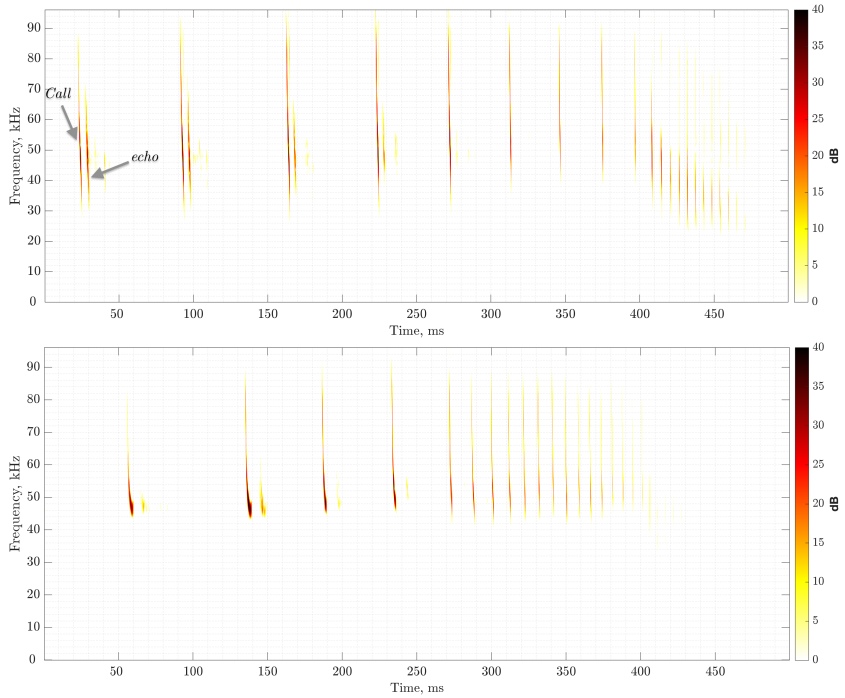

(a) Bat Call Data from the Field Array

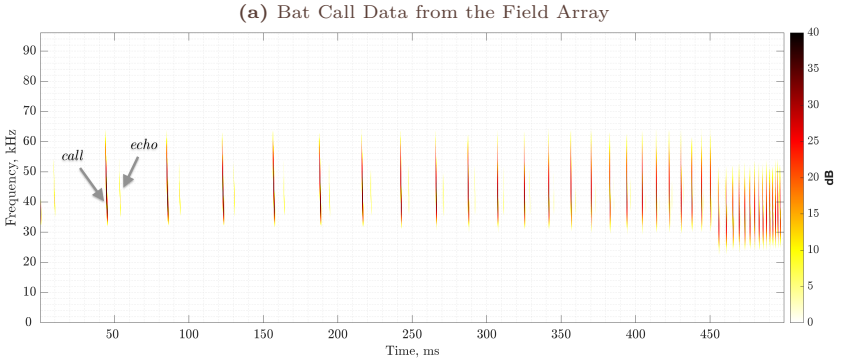

(b) Spectrogram of Simulated Call Sequence

Figure 4: Field and Simulated Primary Data. Comparison between real and simulated echolocation data. (**a**) shows echolocation call sequence data from the field array, the two different species (*Myotis sp.* & *Pipistrellus sp.*) of bats foraging at the experiment site. (**b**) presents a simulated echolocation call-echo sequence as a spectrogram. Note that the echoes in the field data are ground reflections reaching the microphone, not the target echoes reaching the bat as in the simulated sequence.

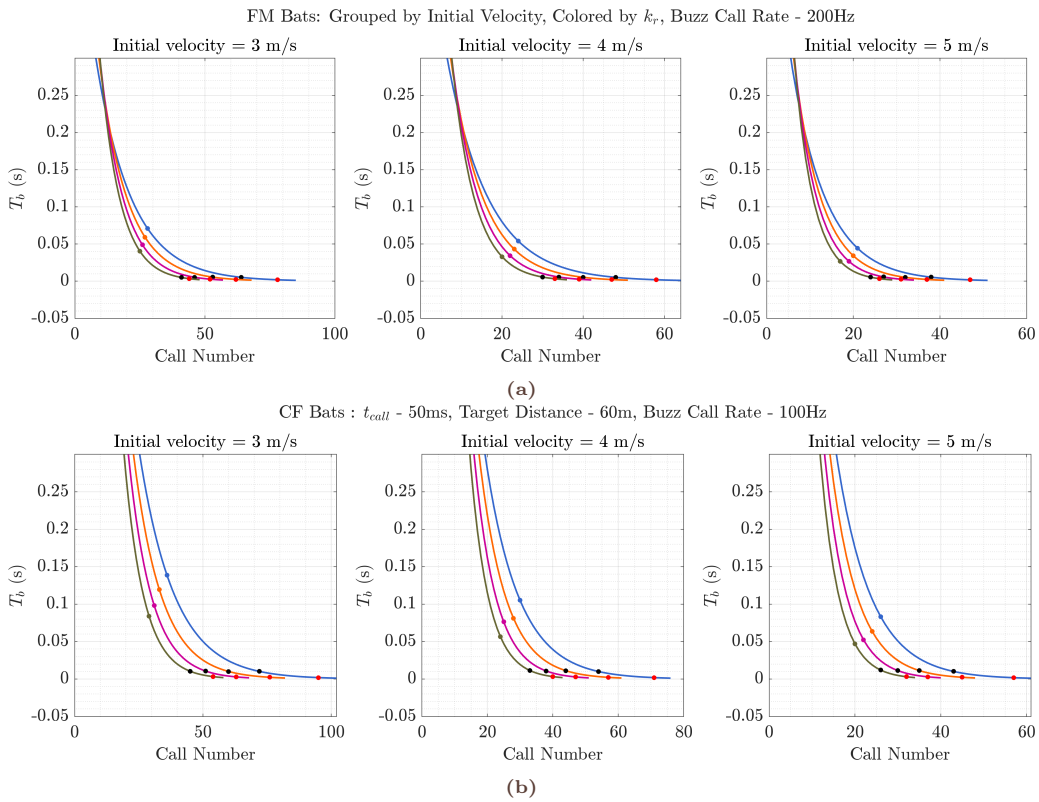

Figure 5: Biological Reaction Time Window. The reaction time window available at every call may be calculated by knowing the biological reaction constant k_r (refer Figure 1b) as $T_b = k_r \times T_a$. The echo delay T_a depends on the bat's velocity relative to the target. Here, T_b is calculated for a range of k_r and relative velocities and the available reaction time at the time of reaching the buzz readiness is marked with a dot of the same colour as the line. The line colours correspond to k_r =4-blue, 5-orange, 6-magenta, 7-olive. The point of maximum call rate is marked by a black dot, and the point of call-echo overlap by a red dot. The top and bottom panels present the results for the FM and CF calls, respectively. The maximum call rate for CF bats is half of that of FM bats. The difference in maximum call rates is known from empirical data. All else being equal, the difference in C_r, max results in a larger time window, but this advantage disappears as the relative velocity increases, as can be seen from a comparison between the top left and bottom right subplots in this figure.

buzz. The bottom panel (Figure 4b) shows a synthetic call sequence from one of the runs of the simulation. The temporal call structure follows the call-echo relationship of the natural echolocation call sequences, ending in a high call rate terminal buzz. The frequency drop is simulated for consistency, but has no bearing on the analyses in the time domain. Note that the variations in call parameters in natural sequences are expected, while the model adheres to strict mathematical definitions. However, the simulated call sequences and the simulation framework serve a central role in deducing the echolocation behaviour of bats in their natural habitats, as the results here indicate.

Figure 5 models the biological reaction time available to an echolocating bat at the time of achieving buzz readiness (or $\mathcal{R}_{max}$) depending on the relative velocity and its biological reaction constant k_r. We deduced the reaction time windows at a range of $k_r = 4, 5, 6, 7$ and $v_r = 3, 4, 5\ m/s$, based on the relationships presented in section 2.1.1 for an FM call and a CF call emitting a foraging bat. Calculated as a k_r multiple of T_a, the echo delay, this time window shrinks with higher relative velocities and higher reaction constants. In the figure, the latter part of the curves is zoomed in to highlight the marked points of buzz readiness, buzz onset and the point where call-echo overlap happens. The bottom panel shows the results for a run with a CF call. The initial distance, maximum call rate, and call duration parameters were adjusted.

Figure 6 visualises the timing of key sonar events during approach: the point of target detection (black line), the onset of call duration contraction (orange line), the peak call rate or buzz readiness (blue line), and the point where call-echo overlap occurs (red line). At slower velocities (1-3 m/s) (panels a, b, c), these events are well-separated, providing a large buffer for sonar adaptation - the responsivity peak and buzz readiness are reached with ample margin, resulting in long buzz sequences. As velocity increases, the time between these events compresses, and in extreme cases, the responsivity threshold is reached after the echo overlap, eliminating the possibility of an effective buzz. In contrast, with increasing velocities (panels d, e, f, g), the sonar update window is compressed. At very high velocities such as 10-15 m/s, as shown in Figures 6f-6h, the responsivity threshold was reached only near or after the point of contact with the target, effectively precluding the production of a structured buzz. The time-to-intercept curve (Figure 1c) explains this trend, showing a hyperbolic decay in available time as velocity increases.

Figure 7 summarises the spatio-temporal dynamic evolving as a combination of relative velocity and biological reaction constant. The fastest reaction time possible, the time left till contact with the target, the available reaction time window and distance to target at the time of achieving buzz readiness shrink as a result of higher relative velocities and slow response. This dynamic affects the outcome of an interception attempt. Notably, the parameter T_{b*} has a narrow range of variation and depends on the call duration at the time of achieving buzz readiness, which decreases with decreasing distance to the target. Therefore, the variation is non-linear. The narrow range of T_{b*} further highlights the importance of modulating velocity, as reducing the relative velocity increases the reaction time window, allowing better sensory update rates.

To understand the above-mentioned spatio-temporal dynamics better, we conducted an extended simulation of 867 pursuit sequences using the model of echolocation in flight with a motile prey. The simulation parameters included an initial approach velocity of 1-30 m/s, a target distance of 20–50 m, reaction constant $k_r = 5$ (corresponding to buzz call rate 200), a source level of 94 dB, and a detection threshold of 20 dB. For each run, we computed the evolving velocity and instantaneous call rate profiles and extracted all valid datapoints ($n = 18646$). These were analysed alongside a comparable dataset from 579 foraging sequences recorded in the field ($n = 6330$).

To characterise the velocity–call rate relationship, we fitted a power-law model of the form

$$v = a \cdot C_r^b,$$

where v is the instantaneous velocity, C_r is the call rate, and a and b are the fit parameters. The regression on simulation data yielded $a = 2.84$ and $b = 0.18$, while the experimental field data produced $a = 9.59$ and $b = -0.15$, both with high statistical significance ($p < 0.0001$) and tight 95% confidence intervals (Figure 8). The sublinear exponent ($b < 1$) in both datasets confirms that bats modulate their sensory sampling rate in a non-linear fashion as velocity increases–i.e., the increase in call rate per unit velocity becomes progressively smaller.

Interestingly, both the simulation and field data revealed weak but significant positive correlations between call rate and velocity, though the strength and structure of the relationship differed. In the simulation, the Spearman correlation was stronger ($r_s = 0.261$), reflecting a controlled, goal-directed approach toward a stationary target in which velocity increased in

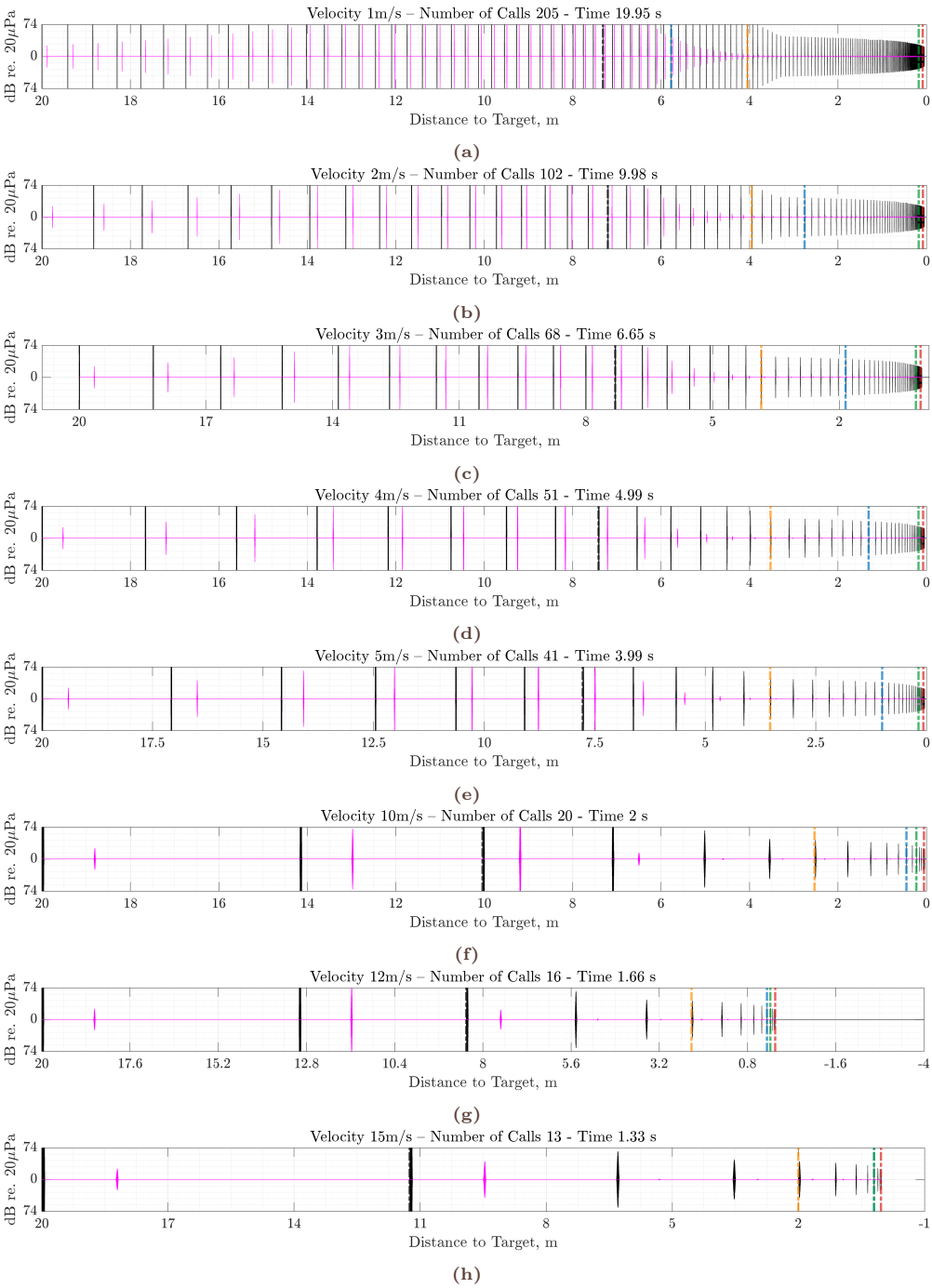

Figure 6: Velocity-Call Rate Tradeoff Each panel corresponds to an initial velocity value in a run of simulated echolocation call sequence. The panel titles also show the corresponding number of calls required to reach the target and the time duration for the entire sequence. A faster approach to the target requires fewer calls. It allows a maximum call rate in closer proximity to the target. The call-echo pairs are coloured in black and magenta, respectively. Event Marker Lines: black - target detection (echo level > 20dB), orange - call duration contraction start, blue - $\mathcal{R}_{max}$, or buzz readiness, green: point of maximum call rate of 200Hz, and red: point where call-echo overlap starts ($T_b = 0$). (See section 2). As the velocity increases, the buzz, as a distinctly identifiable feature, disappears.

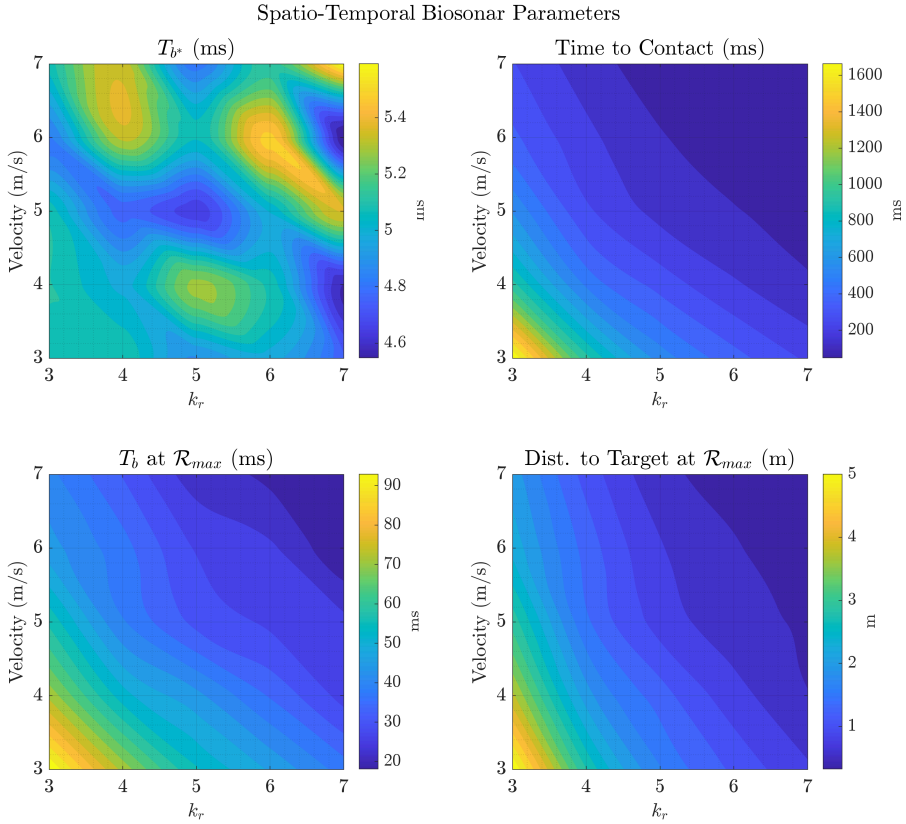

Figure 7: Spatio-Temporal Biosonar Parameters at Velocity and k_r Combinations. The four plots here present the following parameters for combinations of relative velocity and k_r, from top left, clockwise, fastest reaction time T_{b^*}, time to contact, distance to target at the time of buzz readiness and the available reaction time window. The plots highlight that with increasing velocity and slower response (higher k_r), the spatio-temporal parameters shrink, thus affecting the rate of sensory information update and the favourable conditions for a successful interception.

tandem with call rate during the search and approach phases. The fitted power-law function $v = 2.84 \cdot C_r^{0.18}$ reflects this sublinear scaling, suggesting that while velocity rises with increased sampling demand, it does so at a diminishing rate. In contrast, the field data showed a weaker but still significant positive correlation ($r_s = 0.158$), likely due to greater behavioural variability. Field trajectories are expected to include exploratory movement, prey evasive action, and dynamic clutter interactions, all of which introduce noise into the relationship. Notably, high call rates at low velocities—typical of buzz phases—contribute to a flattening or even inversion of the trend locally. Despite this variability, the fitted power law $v = 9.59 \cdot C_r^{-0.15}$ captures the broader structure, reinforcing that predictive velocity–call rate relationships persist across both synthetic and naturalistic behaviour when phase-dependent modulation is considered.

We examined the relationship between flight parameters and acoustic call characteristics across the field dataset of echolocation events (Figure 9). A significant positive correlation was observed between the total distance covered and instantaneous velocity ($r = 0.344$, $p < 0.01$; Figure 9a), indicating that faster trajectories are associated with longer travel distances. Call duration showed a weak but statistically significant positive correlation with velocity in the log-transformed data ($r = 0.128$, $p < 0.0001$; Figure 9b), suggesting a slight tendency for longer calls during higher-speed flight, likely pointing to the initial phases on approaches. In

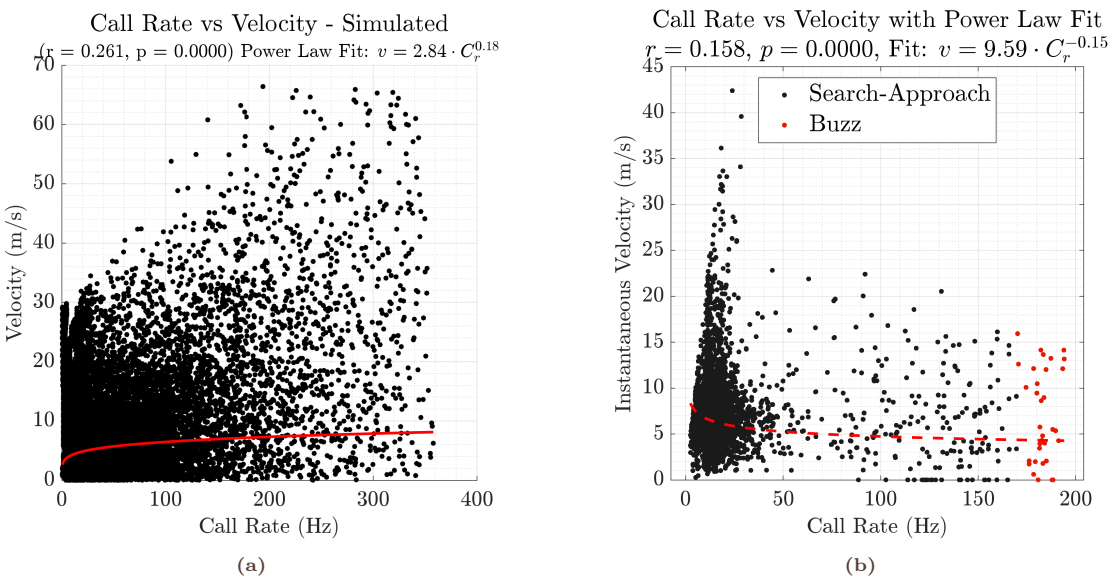

Figure 8: Call Rate vs. Velocity: Comparison between Simulation and Field Data. **8a** Simulation results show a slight positive Spearman correlation between call rate and velocity ($r_s = 0.261$, $p < 0.0001$), consistent with the expectation that bats gradually increase speed while increasing call rate during search and approach. The fitted power-law function (red line) $v = 2.84 \cdot C_r^{0.18}$ indicates a sublinear relationship, meaning that velocity increases with call rate but at a diminishing rate. **(8b)** Field data show a weaker yet significant positive correlation ($r_s = 0.158$, $p < 0.0001$), likely due to behavioural heterogeneity. Buzz sequences (shown in red) exhibit low velocity at higher call rate, an evident velocity-call rate tradeoff. The fitted power-law $v = 9.59 \cdot C_r^{-0.15}$ captures this inverse trend, consistent with the idea that bats slow down while increasing sampling rate during terminal approach. Together, these findings demonstrate how velocity–call rate coordination follows predictable patterns under clean behavioural phases, while real-world variability modulates this structure.

contrast, no meaningful correlation was found between call rate and call duration ($r = -0.014$, $p = 0.2654$; Figure 9c), but a clear distributional clustering that suggested a higher tendency for longer call durations at lower call rates, as may be expected from our posits. However, the log-transformed correlation analysis between the call rate and call duration revealed a significant inverse correlation ($r = -0.434, p < 0.0001$). This pattern arises because the raw (linear) relationship between call rate and call duration is non-linear and heteroscedastic, obscuring the correlation in untransformed data, whereas the log transformation linearises the relationship, revealing the underlying inverse scaling between increasing call rate and decreasing call duration.

We further analysed changes in call duration in relation to local movement patterns. The change in call duration between consecutive calls did not significantly correlate with changes in the distance covered ($r = -0.024$, $p = 0.06$; Figure 9e), nor with the inter-pulse interval (IPI) that followed the call ($r = 0.005$, $p = 0.6959$; Figure 9f). These findings suggest that short-term modulations in call duration are not systematically linked to local positional updates or the timing of subsequent emissions.

The parametric adaptation to call duration and call rate is revealed in the simulated pursuit of a non-stationary prey in figure 10. Every run with the same initial velocity results in a different outcome due to the introduced stochasticity. An example is shown in Figure 10b, where the initial velocity value was set to the mean velocity value of a bat in the field recorded call sequence for comparability. The variability in the time of occurrence of the marked events and the subsequent adaptations to call durations reflect what may be expected in real-world scenarios, as presented in Figure 10a - the model fit to the field data. Notably, the parameter variability becomes more pronounced closer to the target, highlighting the importance of achieving buzz readiness at the

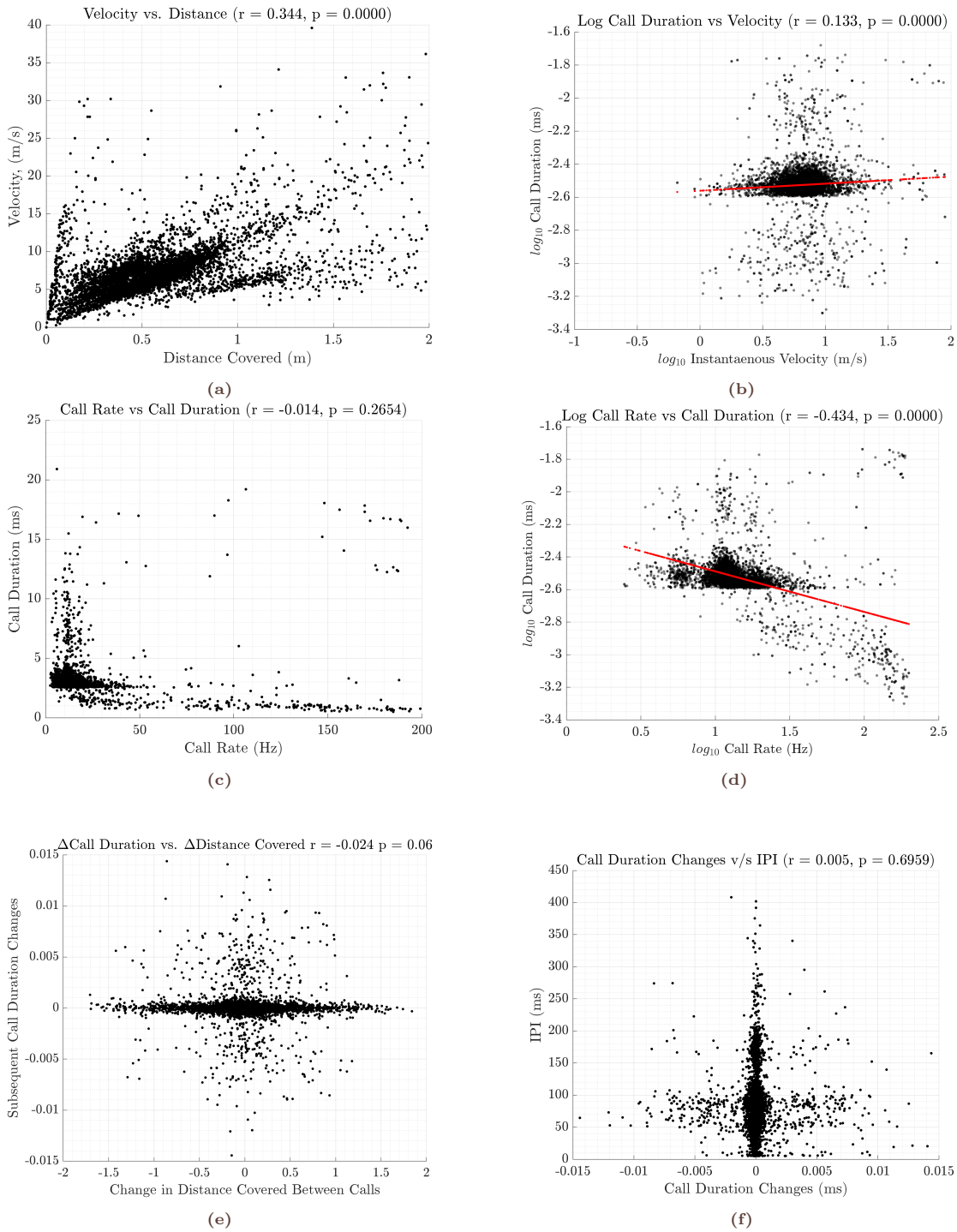

Figure 9: Foraging Flight Echolocation Parameters Relationships among key echolocation parameters across flight sequences. (9a) **Distance vs Velocity**: Inter-call distance increases with flight velocity. (9c) **Call Rate vs Call Duration**: High call rates are constrained to short durations. (9b) **Velocity vs Call Duration**: A modest positive correlation shows that faster flight is associated with slightly longer call durations. (9e) **Change in Call Duration vs Change in Inter-Call Distance**: No consistent relationship - suggesting decoupled control of these parameters. (9f) **Call Duration Changes vs Inter-Pulse Interval (IPI)**: No correlation - Independent adaptations.

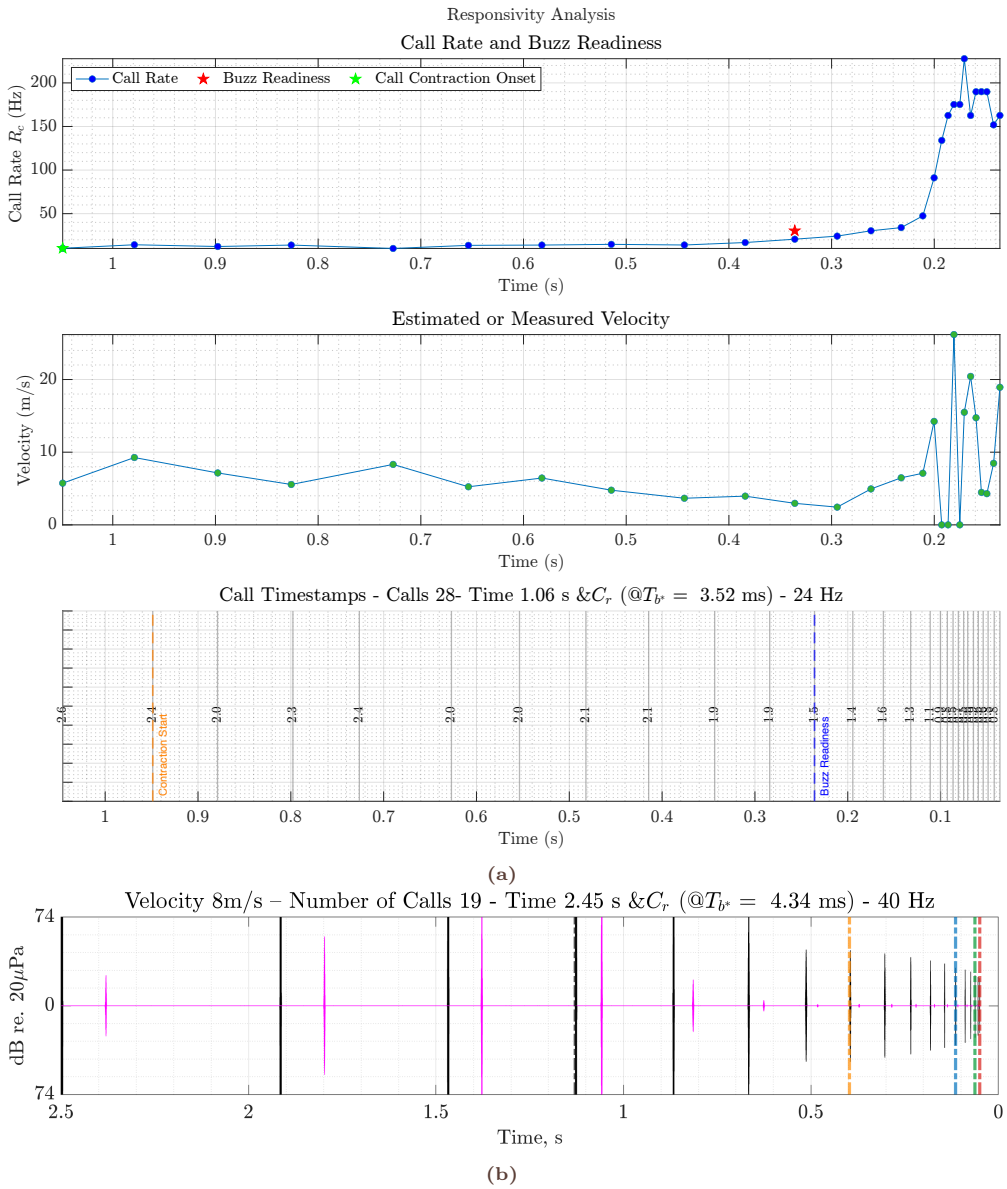

Figure 10: Pursuit of a Motile Prey: Field-Model Comparison. This figure illustrates the application of the responsivity framework to a representative echolocation sequence recorded from free-flying bats. **Top panel:** Call rate R_c (Hz) computed across the entire sequence, with the point of maximum responsivity–termed buzz readiness–marked by a red star. The green star indicates the onset of call duration contraction, automatically estimated from the data. **Second panel:** Estimated velocity profile of the bat, showing fluctuations during the approach and deceleration prior to buzz readiness. **Third panel:** Raw call timestamps represented as vertical bars, with their corresponding call durations annotated. The onset of call duration decrement is marked by an orange vertical line; the buzz readiness point, consistent with the top panel, is marked in blue. **Bottom panel:** A comparable model simulation run using the mean velocity derived from the field sequence. The simulated parameters, including derived T_{b*} and call rate at the buzz readiness point, match the field values closely (T_{b*} = 3.2 ms and C_r = 24 Hz), supporting the model's predictive power. This alignment validates the theoretical framework, showing that responsivity can identify behaviourally relevant thresholds even under noisy, real-world conditions. Together with Figure 2, this example demonstrates the model's robustness in capturing temporal and kinematic sonar adaptations in motile prey pursuit.

earliest possible point. The simulated sequence in Figure 10b, (matched for initial velocity with the field data and target distance 10 m), shows an almost overlap between the point of reaching maximum call rate of 200Hz and the point where the call-echo overlap would begin. Further, for the given velocity profile, the full buzz could not set in without a rapid slowdown. In agreement with the model prediction, the field data show a slowdown from 10 m/s down to 2.4 m/s before accelerating again before the buzz.

Considering the results presented here as a whole, the evolving interplay between the parameters confirms the velocity-call rate tradeoff hypothesis raised in section 2.4.

4 DISCUSSIONS

This study presents a unified theoretical framework linking relative velocity to sonar adaptation in echolocating bats, built upon the concepts of biological reaction time constant and sonar responsivity. Through simulation, analytical modelling, and field recordings, we show that the temporal constraints imposed by relative motion fundamentally govern the bat's capacity to adapt its echolocation call pattern during interception.

Following the equations in section 2, and referring to the models in Figure 1b, with known maximum call rates, the biological reaction constant k_r may be derived. And with known call duration and velocity values, the distance at which the call contraction begins may be predicted, according to Figure 1d.

We gain a key insight into the temporal sequence of physical and biological event series by deducing the fastest biological reaction time as a multiple of echo delay at maximum presumed exertion in an echolocation call sequence. Further, by determining the rate at which the call duration adaptation accelerates, a second-order derivative of the interpulse intervals, the *biosonar temporal responsivity* emerges as a metric of adaptation sharpness, a point from where the emission of buzz becomes physiologically feasible, and the point where the sensory-motor loop is running at it's tightest.

Figure 5 shows how the available time window to prepare for this point of buzz readiness varies with the innate response property and relative velocity. The timing and structure of the simulated buzz sequences correspond closely with findings by Geberl et al.[6], who reported that bats aborted buzzes or shortened their duration when prey was removed shortly before capture, depending on the timing of removal, between 3 and 240 ms. Further, the available time window before contact and the corresponding T_{b^*} as shown in Figure 7 explain the range of time windows as measured in their experiments, the values corresponding to different bat velocities allowing varying length of time to contact. Additionally, recent findings by Jakobsen et al.[16] show a time-normalised echolocation pattern across species, supporting the velocity-tuned responsivity theory proposed in this study.

Our model (Figure 6) predicts that when relative velocity is high, bats may not reach their physiological call rate limit before reaching the target, resulting in truncated or omitted terminal buzz sequences. Conversely, this responsivity peak is reached well ahead of interception at low relative velocities, enabling the bat to emit a long, structured buzz. Further, the results show that buzz readiness shifts closer to the target as velocity increases and typically occurs after call duration contraction has begun, but can occur without the contraction, as shown in figure 6a. In high-velocity approaches, this window collapses, and the bat may be forced to intercept the

target without entering a buzz phase.

Experiments by Geberl et al. [6] show that *Myotis daubentonii* with a buzz call rate of 180–200 Hz, did not initiate a buzz if prey was removed more than 150 ms before interception. This behavior maps onto our modeled scenarios where $v \approx 2 - 3\,\mathrm{m/s}$ and $k_r = 4$–5, with buzz readiness reached prior to buzz onset (Figures 1b, 5 & 7), more specifically the time windows before interception. Their findings also align with our prediction that even late prey removal (<20 ms) before contact) results in capture abandonment, i.e., the bats are still able to respond and adapt, consistent with the predictions of our model that any perturbations above the reaction threshold $T_{b^*} \approx 5$ ms will register a response. Further, they report that very late prey removals (≈3 ms before expected contact time) resulted in continued full buzz II sequence, which can be explained as the perturbation occurring under the reaction limit. Their speculation of a *point of no return* is the event occurring faster than the fastest reaction time a bat could achieve. From their experiments, it may be deduced that the fastest the *Myotis daubentonii* can reaction is somewhere in the range of few milliseconds. This spatiotemporal dynamic, represented in Figure 7, and the model fit in Figure 10 explain such a circumstantial outcome.

Together, these results reframe the buzz not as a discrete behavioural unit but as a consequence of operating at the upper bound of temporal responsiveness. This interplay gives credence to the central hypothesis of our work - that the velocity-call rate tradeoff is at the centre of an evolving interception strategy. Our results (Figure 8 & 9) from the field study support this further. As shown in Figure 9a, bats increase the spatial gap between calls with velocity, maintaining a consistent sampling density. While changes in inter-call distance do not directly predict subsequent call duration changes (Figure 9e), a modest positive correlation is observed between velocity and call duration (Figure 9b). Critically, high call rates are exclusively paired with short call durations (Figure 9c). To assess whether temporal adjustments in call structure follow changes in signal duration, we examined the relationship between call duration changes and the inter-pulse interval (Figure 9f). The correlation was negligible ($r = 0.005$, $p = 0.6959$), indicating no consistent pattern. This suggests that separate mechanisms control duration modulation and call timing. The absence of coupling between these two parameters implies a degree of behavioural independence - a voluntary decision to adjust call duration.

The example presented in Figure 10 highlights the applicability of the responsivity model to naturalistic foraging behaviour. Despite variability in velocity and target location, the model robustly identifies the buzz readiness point, as confirmed by the convergence of responsivity maxima and call rate acceleration in the field data. The observed alignment between model predictions and empirical measures, both in T_{b^*} and call rate, demonstrates the framework's ability to uncover latent sensorimotor thresholds. Notably, the early onset of call duration contraction relative to the buzz readiness point suggests a pre-emptive adjustment strategy, consistent with the hypothesis that echolocating bats operate within anticipatory control regimes. The fastest reaction time, T_{b^*} calculated from the field data, at 3.52 ms matches the results observed by Gerberl et. al. (2015) [6], reporting response by buzz shortening or abandonment, to prey removal <20 ms (within 6 cm target distance) before the expected contact time, in aerial hawking *Myotis daubentonii*. These results reinforce the utility of responsivity as a predictive marker and support its use in analysing real-world biosonar dynamics under natural constraints (See below).

The experiments performed by Wohlgemuth & Moss (2013) [7] with *Eptesicus fuscus* where

multiple targets of varying velocities were presented to a stationary subject and the sonar parameters were analysed to identify the signatures for target selection, they report that the higher velocity targets elicited an earlier adjustment in call duration and interval. In contrast, these adjustments occurred later when the bat chose to track the slower-moving targets. Further, in the presence of distractor objects closer, the bats adjusted their call duration to the nearest object, followed by a further decrement when the target crossed the distractor and approached the bat (Figure 2 & 4 in [7]). The call duration fluctuations outputs from simulating a motile prey in our study match the field-measured patterns as in Figure 10a. Further validation comes from Jakobsen et al. (2025) [16]. The data presented in Figure 1 of their study shows the velocity-call rate tradeoff, where flight speed decreases as the call intervals (i.e., increasing call rate) decrease closer to the target.

A key assumption of the present model is that the echolocation call rate can be modulated in response to relative velocity, independent of biomechanical constraints such as wingbeat. Traditional hypotheses proposed that call emission in bats is tightly coupled to the wingbeat cycle, potentially limiting adaptive flexibility in call rate. However, recent work by Xia et al. (2025) [21] provides strong behavioural evidence that this coupling is highly flexible. Their study showed that while many species maintain phase-locked call-wingbeat patterns during early approach phases, this coupling is frequently broken during high-rate sequences such as terminal buzzes. The decoupling becomes especially apparent in cluttered environments and during prey tracking, indicating that sonar demands can override biomechanical rhythm.

Complementing this behavioural evidence, the physiological limits of call rate are now better understood by identifying superfast laryngeal muscles in vespertilionid bats. Elemans et al. [22] demonstrated that these muscles can sustain cyclic contractions up to 190–200 Hz, aligning precisely with the call rates observed during the buzz phase. Importantly, their findings showed that the maximum call rate is not constrained by call–echo overlap, as echoes typically terminate well before the next call. Instead, the limit is set by the neuromuscular kinetics of the vocal apparatus. These findings confirm that bats are not only behaviorally capable of decoupling calls from wingbeats but also physiologically equipped with superfast muscles that enable rapid vocal production when adaptive sonar feedback is most critical.

The extended simulation of a CF bat, characterised by longer-duration echolocation calls (50 ms) and a buzz rate of 100 Hz, reveals important refinements to the model's predictions. Despite the inherently longer call durations, the results show that buzz readiness is achieved well before the onset of the terminal buzz. (Figure 5b). However, in this simulation, the call duration contraction led to calls being significantly shorter at the time of the buzz, by 1% of the intial duration of 50 ms, and at the point of maximum responsivity 28%, whereas the call duration contraction in CF bats is not that drastic but a typical factor of 10, which implies a significant call-echo overlap without extensive call contractions. However, as it has been studied, the CF bats show compensatory behaviour to the Doppler shift phenomenon [12, 23, 24], and can shift calling frequencies in anticipation of target-reach [14, 25] and it is advantageous with increasing Δf as the velocity increases (Supplementary. Figure 11). Thus, maintaining a higher relative velocity becomes an underlying necessity, an interception strategy based on persistently higher relative velocities, for a successful interception to maintain the frequency domain advantage, as the higher relative velocities resolve the call-echo better due to the Doppler effect. Field observations and experimental studies report that CF bats are particularly faster and more

efficient hunters [26, 27].

This demonstrates that call duration, while relevant, is not the dominant constraint on buzz onset timing. Instead, the model reaffirms that relative velocity and biological reaction time quantified via sonar responsivity are the primary variables governing the dynamics of interception. Although the CF bat does not achieve the extreme call rates typical of FM bats during the terminal phase, the trajectory of its sensory adaptation still conforms to the model's velocity-constrained prediction. This indicates that differing acoustic strategies may converge on similar responsivity limits, modulated by species-specific neural latencies and signal-processing capacities.

Furthermore, the ability of CF bats to reach buzz readiness without overlapping calls and echoes, albeit in the frequency domain, suggests a compensatory mechanism through which longer-duration signals can coexist with effective sensory-motor control. Such flexibility could reflect evolutionary tradeoffs that enable CF bats to exploit distinct ecological niches [28, 29]. If reaction time limits are harder to compress due to the intrinsic properties of the auditory system, bats may compensate by altering flight velocity profiles or shifting foraging strategies altogether, or, as the recent experimental evidence suggests, oscillating ears might offer a solution [30]. These results underscore the role of sensory constraints as a fundamental driver of behavioural and ecological divergence and highlight the model's potential to elucidate the evolutionary pressures shaping biosonar systems across taxa.

To further explore the key predictions of this framework, we propose future experiments using augmented echo-acoustic reality via real-time echo manipulation *ad aures*. Decoupling physical distance from echo delay and simulating prey with controlled relative velocities makes it possible to induce or suppress buzz readiness conditions. Combined with onboard inertial sensors and neural recordings, these experiments could provide direct, real-time evidence of how bats modulate responsivity and structure their sonar output as a function of dynamically evolving interception parameters.

In summary, this work introduces a reaction time-constrained model of echolocation behaviour that explains when and why bats restructure their call sequences during prey pursuit. The results unify a range of previously observed behaviours - shortening, omission, and early termination of buzz- under a single framework, offering a predictive theory of sonar adaptation in the context of motion.

5 CONCLUSIONS

This study presents a mechanistic framework that connects prey interception behaviour in echolocating bats to relative velocity through the lens of sonar responsivity and reaction time. Crucially, by identifying the point where the acceleration in call rate converges to the remaining gap toward the maximum call rate, we capture the moment of *buzz readiness*—a threshold defined by the physiological constraint of the bat's reaction time. This definition leverages a purely mathematical condition derived from observed timings, without requiring knowledge of the bat's position or speed.

Quantitative analysis of simulated and empirical data demonstrates a consistent power-law relationship between velocity and call rate, indicating a fundamental tradeoff in sensory update capacity. This relationship supports the studies that show bats modulate their echolocation

effort non-linearly in response to kinematic demands.

The results validate the model's predictive power and explain observed behaviours, such as buzz omission and capture abandonment, as rational outcomes of temporal and energetic constraints. Experimental work by Geberl et al. and recent findings by Jakobsen et al. align well with the theory, providing strong empirical support. Thus, traditionally interpreted only in behavioural or acoustic terms, the sonar pulse train can now be seen as a time-series readout of the bat's sensorimotor state. This enables a powerful approach to studying neural and behavioural transitions using only a single-microphone recording and a known or assumed maximum call rate. The capacity to infer reaction constraints, behavioural phase transitions, and adaptive sensory thresholds from call time data underscores the exceptional analytic leverage of temporal sonar patterns in echolocation research.

Finally, this framework lays the foundation for future experiments using real-time echo manipulation to test adaptive strategies under controlled conditions. Together, these contributions advance the understanding of how biological systems optimise perception and action under velocity-dependent constraints, offering a generalisable model for dynamic sensory-motor integration.

AUTHORS' NOTE

We fondly refer to the simulated bats as *Vespertillio numeralis* and *Rhinolophus imaginaria* – species native to the domain of simulation.

AUTHOR CONTRIBUTIONS

RU conceived the responsivity framework, developed the theoretical and mathematical models, programmed and executed the simulations, designed and constructed the field recording system and associated software, performed the field experiments, analysed the complete dataset, and wrote the manuscript. UF advised on the development and execution of the field experiments, reviewed experimental protocols, secured funding for the fieldwork, revised the manuscript, and contributed to technical refinements throughout the study.

ACKNOWLEDGEMENTS

We extend our gratitude to our colleagues at the Technical University of Munich (TUM) for their valuable discussions and constructive feedback throughout the course of this work. We thank Christian Fink for technical assistance with builing the field array.

COMPETING INTEREST

The authors declare no competing interests.

FUNDING

A part of the DFG Grant WI1518/18-1 supported the funding for the field study.

DATA AND RESOURCE

The simulation code, experimental data, and analysis scripts will be made available upon publication. Requests for access to data and code during the review process may be directed to the author via email.

Manuscript Information

Version: R3
Last updated: June 16, 2025
Words in text: 7737
Words outside text (captions, etc.): 1216
Number of floats/tables/figures: 11
Number of math displayed: 19

REFERENCES

1. Griffin, D. R. & Galambos, R. The Sensory Basis of Obstacle Avoidance by Flying Bats. *Journal of Experimental Zoology* **86,** 481–506. ISSN: 1097-010X. https://onlinelibrary.wiley.com/doi/abs/10.1002/jez.1400860310.
2. Griffin, D. R., Webster, F. A. & Michael, C. R. The Echolocation of Flying Insects by Bats. *Animal Behaviour* **8,** 141–154. ISSN: 0003-3472. https://www.sciencedirect.com/science/article/pii/0003347260900221.
3. Griffin, D. R. How Bats Guide Their Flight by Supersonic Echoes. *American Journal of Physics* **12,** 342–345. ISSN: 0002-9505. https://aapt.scitation.org/doi/10.1119/1.1990634.
4. Griffin, D. R. Return to the Magic Well: Echolocation Behavior of Bats and Responses of Insect Prey. *BioScience* **51,** 555–556. ISSN: 0006-3568. https://doi.org/10.1641/0006-3568(2001)051[0555:RTTMWE]2.0.CO;2.
5. Moss, C. F. & Surlykke, A. Auditory Scene Analysis by Echolocation in Bats. *The Journal of the Acoustical Society of America* **110,** 2207–2226. ISSN: 0001-4966. pmid: 11681397.
6. Geberl, C., Brinkløv, S., Wiegrebe, L. & Surlykke, A. Fast Sensory–Motor Reactions in Echolocating Bats to Sudden Changes during the Final Buzz and Prey Intercept. *Proceedings of the National Academy of Sciences* **112,** 4122–4127. https://www.pnas.org/doi/full/10.1073/pnas.1424457112.
7. Wohlgemuth, M. & Moss, C. Active Listening in a Complex Environment. *Proceedings of Meetings on Acoustics* **19,** 010030. ISSN: 1939-800X. https://doi.org/10.1121/1.4800959.
8. Moss, C. F. & Surlykke, A. Probing the Natural Scene by Echolocation in Bats. *Frontiers in Behavioral Neuroscience* **4.** ISSN: 1662-5153. https://www.frontiersin.orghttps://www.frontiersin.org/journals/behavioral-neuroscience/articles/10.3389/fnbeh.2010.00033/full.
9. Jakobsen, L. & Surlykke, A. Vespertilionid Bats Control the Width of Their Biosonar Sound Beam Dynamically during Prey Pursuit. *Proceedings of the National Academy of Sciences* **107,** 13930–13935. ISSN: 0027-8424. pmid: 20643943.
10. Wilson, A. M. *et al.* Locomotion Dynamics of Hunting in Wild Cheetahs. *Nature* **498,** 185–189. ISSN: 1476-4687. https://www.nature.com/articles/nature12295.
11. Perrine, J. O. The Doppler and Echo Doppler Effect. *American Journal of Physics* **12,** 23–28. ISSN: 0002-9505, 1943-2909. http://aapt.scitation.org/doi/10.1119/1.1990527.
12. Trappe, M. & Schnitzler, H. .-. Doppler-Shift Compensation in Insect-Catching Horseshoe Bats. *Naturwissenschaften* **69,** 193–194. ISSN: 0028-1042, 1432-1904. http://link.springer.com/10.1007/BF00364902.
13. Bell, G. P. & Fenton, M. B. The Use of Doppler-shifted Echoes as a Flutter Detection and Clutter Rejection System: The Echolocation and Feeding Behavior of Hipposideros Tuber (Chiroptera :Hipposideridae). *Behav Ecol Sociobiol,* 109–114.
14. Schoeppler, D., Kost, K., Schnitzler, H.-U. & Denzinger, A. Transmitter and Receiver of the Low Frequency Horseshoe Bat Rhinolophus Paradoxolophus Are Functionally Matched for Fluttering Target Detection. *Journal of Comparative Physiology. A, Neuroethology, Sensory, Neural, and Behavioral Physiology* **209,** 191–202. ISSN: 0340-7594. pmid: 36136120. https://www.ncbi.nlm.nih.gov/pmc/articles/PMC9898408/.
15. Yoshida, S., Hase, K., Heim, O., Kobayasi, K. I. & Hiryu, S. Doppler Detection Triggers Instantaneous Escape Behavior in Scanning Bats. *iScience,* 109222. ISSN: 25890042. https://linkinghub.elsevier.com/retrieve/pii/S2589004224004437.

16. Jakobsen, L. *et al.* Velocity as an Overlooked Driver in the Echolocation Behavior of Aerial Hawking Vespertilionid Bats. *Current Biology,* S096098222401710X. ISSN: 09609822. https://linkinghub.elsevier.com/retrieve/pii/S096098222401710X.

17. Mulla, D. M. & Keir, P. J. Neuromuscular Control: From a Biomechanist's Perspective. *Frontiers in Sports and Active Living* **5.** ISSN: 2624-9367. https://www.frontiersin.org/journals/sports-and-active-living/articles/10.3389/fspor.2023.1217009/full.

18. Zago, M., McIntyre, J., Senot, P. & Lacquaniti, F. Visuo-Motor Coordination and Internal Models for Object Interception. *Experimental Brain Research* **192,** 571–604. ISSN: 1432-1106. pmid: 19139857.

19. *Biosonar* (eds Surlykke, A., Nachtigall, P. E., Fay, R. R. & Popper, A. N.) ISBN: 978-1-4614-9145-3 978-1-4614-9146-0. http://link.springer.com/10.1007/978-1-4614-9146-0 (Springer New York, New York, NY).

20. Ester, M., Kriegel, H.-P., Sander, J. & Xu, X. A Density-Based Algorithm for Discovering Clusters in Large Spatial Databases with Noise. *Proceedings of 2nd International Conference on Knowledge Discovery and Data Mining* **(KDD-96).**

21. Xia, H., Ma, N., Li, A. & Luo, J. Call Production and Wingbeat Coupling Is Flexible and Species-Specific in Echolocating Bats. *Annals of the New York Academy of Sciences* **1547,** 105–115. ISSN: 1749-6632. https://onlinelibrary.wiley.com/doi/abs/10.1111/nyas.15325.

22. Elemans, C. P. H., Mead, A. F., Jakobsen, L. & Ratcliffe, J. M. Superfast Muscles Set Maximum Call Rate in Echolocating Bats. *Science* **333,** 1885–1888. ISSN: 0036-8075. pmid: 21960635.

23. Schuller, G. The Role of Overlap of Echo with Outgoing Echolocation Sound in the Bat Rhinolophus Ferrumequinum. *Naturwissenschaften* **61,** 171–172. ISSN: 1432-1904. https://doi.org/10.1007/BF00602598.

24. Schuller, G. Echo Delay and Overlap with Emitted Orientation Sounds and Doppler-Shift Compensation in the Bat,Rhinolophus Ferrumequinum. *Journal of comparative physiology* **114,** 103–114. ISSN: 1432-1351. https://doi.org/10.1007/BF00656811.

25. Hiryu, S., Shiori, Y., Hosokawa, T., Riquimaroux, H. & Watanabe, Y. On-Board Telemetry of Emitted Sounds from Free-Flying Bats: Compensation for Velocity and Distance Stabilizes Echo Frequency and Amplitude. *Journal of Comparative Physiology A* **194,** 841–851. ISSN: 1432-1351. https://doi.org/10.1007/s00359-008-0355-x.

26. Lazure, L. & Fenton, M. B. High Duty Cycle Echolocation and Prey Detection by Bats. *Journal of Experimental Biology* **214,** 1131–1137. ISSN: 1477-9145, 0022-0949. https://journals.biologists.com/jeb/article/214/7/1131/33546/High-duty-cycle-echolocation-and-prey-detection-by.

27. Fenton, M. B., Faure, P. A. & Ratcliffe, J. M. Evolution of High Duty Cycle Echolocation in Bats. *Journal of Experimental Biology* **215,** 2935–2944. ISSN: 1477-9145, 0022-0949. https://journals.biologists.com/jeb/article/215/17/2935/10996/Evolution-of-high-duty-cycle-echolocation-in-bats.

28. Obrist, M. K., Fenton, M. B., Eger, J. L. & Schlegel, P. A. What Ears Do for Bats: A Comparative Study of Pinna Sound Pressure Transformation in Chiroptera. *The Journal of experimental biology* **180,** 119–52. ISSN: 0022-0949. pmid: 8371084.

29. Denzinger, A., Tschapka, M. & Schnitzler, H.-U. The Role of Echolocation Strategies for Niche Differentiation in Bats. *Canadian Journal of Zoology* **96,** 171–181. ISSN: 0008-4301. https://cdnsciencepub.com/doi/10.1139/cjz-2017-0161.

30. Umadi, R. *Oscillating Ears Dynamically Transform Echoes in Constant-Frequency Bats* https://www.biorxiv.org/content/10.1101/2025.06.14.659613v1. Pre-published.